Acta Polytechnica **53**(Supplement):646–651, 2013
doi:10.14311/AP.2013.53.0646

available online at http://ojs.cvut.cz/ojs/index.php/ap

ARGO-YBJ: STATUS AND HIGHLIGHTS

Giuseppe Di Sciascio*, on behalf of the ARGO-YBJ Collaboration

INFN – Sezione di Roma Tor Vergata, Viale della Ricerca Scientifica 1, I-00133 Roma
* corresponding author: disciascio@roma2.infn.it

Abstract. The ARGO-YBJ experiment has been gathering data steadily since November 2007 at the YangBaJing Cosmic Ray Laboratory (Tibet, P.R. China, 4300 m a.s.l., 606 g/cm^2). ARGO-YBJ is confronting various open problems in Cosmic Ray (CR) physics. The search for CR sources is carried out by observing TeV gamma-ray sources, both galactic and extra-galactic. The CR spectrum, composition and anisotropy are measured in a wide energy range (TeV ÷ PeV), thus overlapping direct measurements for the first time. This paper summarizes the current status of the experiment and describes some of the scientific highlights since 2007.

Keywords: cosmic rays, extensive air showers, gamma-ray astronomy.

1. Introduction

Exploiting the full coverage approach at high altitude, the ARGO-YBJ experiment is an air shower array able to detect cosmic radiation with an energy threshold of a few hundred GeV. The detector has been gathering data steadily since November 2007 with a duty cycle larger than 86 %. The trigger rate is 3.5 kHz. The detector characteristics and performance are described in detail in [1, 2]. The main results obtained by ARGO-YBJ are described in [3]. This paper summarizes the status of the experiment and reviews some highlights.

2. Gamma-ray astronomy

From November 2007 the ARGO-YBJ experiment collected about 4×10^{11} events in 1543 days of total effective observation time. Five known VHE γ-ray sources were detected with a statistical significance greater than 5 standard deviations (s.d.), i.e. Crab Nebula, Mrk421, Mrk501, MGRO J1908+06 and MGRO J2031+41. A number of flares from Mrk421 and Mrk501 were observed and studied in detail. Evidence of TeV flaring activity from the Crab Nebula in coincidence with AGILE/Fermi observations is also reported. Details on the analysis procedure (e.g., data selection, background evaluation, systematic errors) are discussed in [4, 5].

2.1. Crab Nebula

With all the data recorded in 3.5 years ARGO-YBJ observed a TeV signal from the Crab Nebula with a statistical significance of about 17 s.d., proving that the cumulative sensitivity of the detector was 0.3 Crab units.

The observed flux is consistent with steady emission, and the observed differential energy spectrum in the 0.330 TeV range can be described by $\mathrm{d}N/\mathrm{d}E = (3.0 \pm 0.30) \times 10^{-11}\,(E/\mathrm{TeV})^{-2.57\pm0.09}$ photons cm^{-2} s^{-1} TeV^{-1}, in good agreement with other observations. According to MC simulations, 84 % of the detected events come from primary photons with energies greater than 300 GeV, while only 8 % come from primaries above 10 TeV. We evaluate systematic error on the flux less than 30 %, mainly due to the background estimaation and to the uncertainty on the absolute energy scale.

According to the AGILE and Fermi data, 4 major flaring episodes at energies $E > 100$ MeV occurred during ARGO-YBJ data acquisition [6–9].

Flare 1 Starting time MJD 54857 (Feb. 2009), duration $\Delta t \sim 16$ days, maximum flux $F_{\max} \sim 5$ times larger than the steady flux [7]. During this flare no excess is present in our data, for any multiplicity threshold.

Flare 2 Starting time MJD 55457 (Sept. 2010), duration $\Delta t \sim 4$ days, maximum flux $F_{\max} \sim 5$ times larger than the steady flux [6, 7]. According to temporal data analysis, the γ-ray emission is concentrated in 3 narrow peaks of ∼ 12 hours duration each [8, 10]. Integrating the 3 transits we observe for $N_{\mathrm{pad}} > 40$ an excess of 3.1 s.d. over the expected steady flux (0.55 s.d.). If the excess were due to a flare, the γ-ray flux would be higher by a factor of ∼ 5 with respect to the steady flux at energies around 1 TeV. Integrating the data over 10 transits (from MJD 55456/57 to MJD 55465/66) the signal significance is 4.1 s.d. (pre-trial), while 1.0 s.d. is expected from the steady flux [11]. No measurement from Cherenkov telescopes is available in coincidence with our observations and in coincidence with the various spikes to confirm this excess. Sporadic measurements performed by the MAGIC and VERITAS telescopes at different times from MJD 55456.45 to MJD 55459.49 show no evidence for flux variability [12, 13].

Flare 3 Starting time MJD 55660 (Apr. 2011) [14], duration $\Delta t \sim 6$ days, maximum flux $F_{\max} \sim 14$

times larger than the steady flux [8]. Integrating the ARGO-YBJ data over the 6 days in which AGILE detected a flux enhancement, i.e. from MJD 55662 to MJD 55668, we find evidence for an excess for events with $N_{\rm pad} > 100$ at a level of about 3.5 s.d. No measurement from Cherenkov telescopes is available during these days, due to the presence of the Moon during the Crab transits.

Flare 4 Starting time MJD 56111 (July 3, 2012) [9], duration $\Delta t \sim 3$ days. The daily-averaged emission doubled from $(2.4 \pm 0.5) \times 10^{-6}\,\mathrm{ph\,cm^{-2}\,s^{-1}}$ on July 2 to $(5.5 \pm 0.7) \times 10^{-6}\,\mathrm{ph\,cm^{-2}\,s^{-1}}$ on July 3. A preliminary analysis of the ARGO-YBJ data shows an excess of events with statistical significance of about 4 s.d. from a direction consistent with the Crab Nebula on July 3, corresponding to a flux ≈ 8 times higher than the average emission at a median energy of ~ 1 TeV [15]. The expected steady flux corresponds to 0.33 s.d. No significant excess is detected in the following days from July 4 to 6. Once again, no measurement from Cherenkov telescopes is available during these days.

In conclusion, the ARGO-YBJ data show marginal evidence of a TeV flux increase correlated to the MeV÷GeV flaring activity, with insufficient statistical significance to draw a firm conclusion (the post-trial probability is of order 10^{-3} for each flare). Nevertheless, the probability of observing 3 flares out of 4 in coincidence with the satellites by chance is very low. A detailed analysis of the Crab Nebula TeV emission is under way, and a paper is in preparation.

2.2. Blazar Mrk421

ARGO-YBJ is monitoring Mrk421 above 0.3 TeV, studying the correlation of the TeV flux with X-ray data. We observed this source with a total significance of about 14 s.d., averaging over quiet and active periods. It is well known that this AGN is characterized by strong flaring activity both in X-rays and in TeV γ-rays. Many flares are observed simultaneously in both bands. The γ-ray flux observed by ARGO-YBJ has a clear correlation with the X-ray flux. No lag between X-ray and γ-ray photons longer than 1 day is found. The evolution of the spectral energy distribution (SED) is investigated by measuring spectral indices at four different flux levels. Spectral hardening is observed in both X-ray and γ-ray bands. The γ-ray flux increases quadratically with the simultaneously measured X-ray flux. All these observational results strongly favor the Self-Synchro Compton (SSC) process as the underlying radiative mechanism. The results of Mrk421 long-term monitoring are summarized in [16].

2.3. Blazar Mrk501

The long-term observation of the Mrk501 TeV emission by ARGO-YBJ can be described by the following differential energy spectrum:

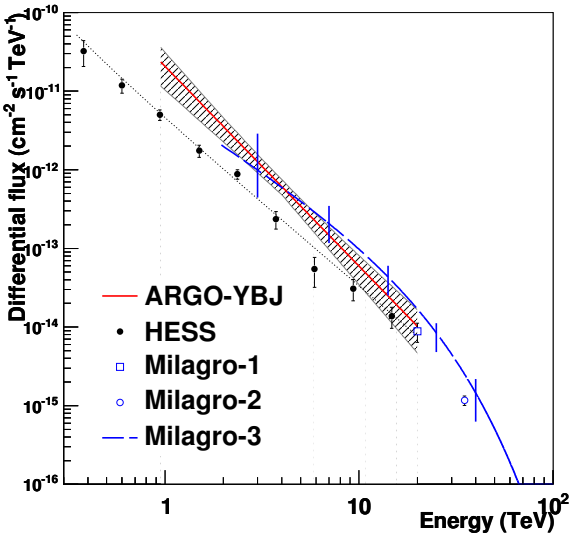

FIGURE 1. Gamma-ray flux from MGRO J1908+06 measured by ARGO-YBJ (red line) compared to other measurements. The dashed area represents the 1 s.d. error. The plotted errors are purely statistical for all the detectors. For details and references, see [18].

$\mathrm{d}N/\mathrm{d}E = (1.92 \pm 0.44) \times 10^{-12}\,(E/2\mathrm{TeV})^{-2.59\pm0.27}$ $\mathrm{ph\,cm^{-2}\,s^{-1}\,TeV^{-1}}$, corresponding to 0.312 ± 0.076 Crab units above 1 TeV.

The largest flare since 2005 started in October 2011. During the brightest γ-ray flaring episodes from October 17 to November 22, 2011, an excess of the event rate over 6 s.d. was detected by ARGO-YBJ, corresponding to an increase of the γ-ray flux above 1 TeV by a factor of 6.6 ± 2.2 from its steady emission [17]. During the flare, the differential flux is $\mathrm{d}N/\mathrm{d}E = (2.92 \pm 0.52) \times 10^{-12}\,(E/4\mathrm{TeV})^{-2.07\pm0.21}$ photons $\mathrm{cm^{-2}\,s^{-1}\,TeV^{-1}}$, corresponding to 2.05 ± 0.48 Crab units above 1 TeV. Remarkably, γ-rays with energies above 8 TeV are detected with statistical significance of about 4 s.d., which had not happened since the 1997 flare. The average SED for steady emission is well described by a simple one-zone SSC model. However, the detection of γ-rays above 8 TeV during the flare challenges this model due to the hardness of the spectra [17].

2.4. MGRO J1908+06

The γ-ray source MGRO J1908+06 was discovered by Milagro at a median energy of ~ 20 TeV and confirmed by HESS at energies above 300 GeV. The Milagro and HESS energy spectra are in disagreement, the Milagro result being higher by a factor of about 3 at 10 TeV.

ARGO-YBJ observed a TeV emission from MGRO J1908+06 with a maximum significance of about 7.3 s.d. for $N_{\rm pad} \geq 20$ in 6867 hours on-source [18]. The intrinsic extension is determined to be $\sigma_{\rm ext} = 0.49^\circ \pm 0.22$, consistent with the HESS measurement ($\sigma_{\rm ext} = 0.34^{\circ\,+0.04}_{-0.03}$). The best fit spectrum obtained is:

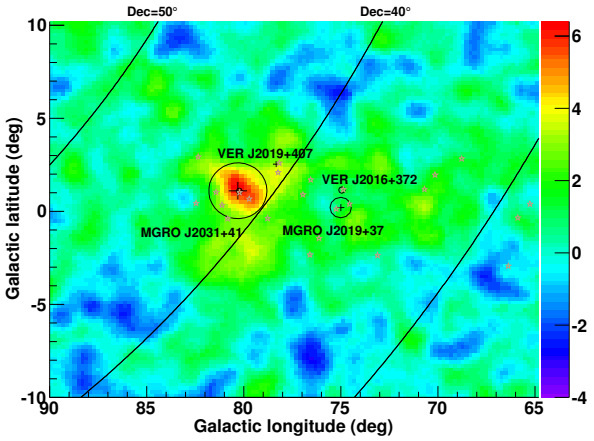

Figure 2. Significance map of the Cygnus region as observed by ARGO-YBJ for $N_{\rm pad} > 20$. The four known VHE γ-ray sources are reported. The errors on the MGRO source positions are marked with crosses, while the circles indicate their intrinsic sizes. The cross for VER J2019+407 indicates its extension. The source VER J2016+372 is marked with a small circle without position errors. The small circle within the errors of MGROJ2031+41 indicates the position and extension of source TeV J2032+4130, as estimated by the MAGIC collaboration. The open stars mark the location of the 24 GeV sources in the second *Fermi* LAT catalog. For details and references, see [19].

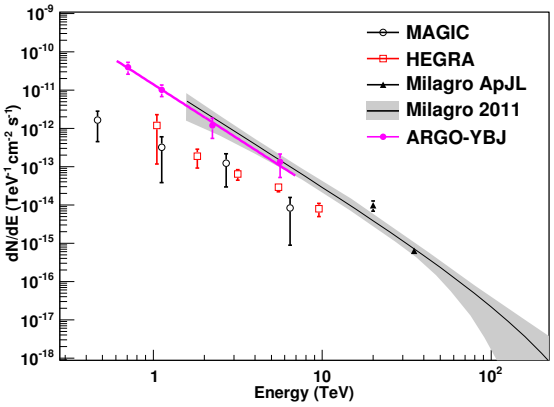

Figure 3. Energy spectrum of MGRO J2031+41/TeV J2032+4130 as measured by ARGO-YBJ (magenta solid line). The spectral measurements of HEGRA and MAGIC are also reported for comparison. The solid black line and the shaded area indicate the differential energy spectrum and the 1 s.d. error region, as recently determined by the Milagro experiment. The two triangles give the previous flux measurements by Milagro at 20 TeV and 35 TeV. For details and references, see [19].

$\mathrm{d}N/\mathrm{d}E = (6.1 \pm 1.4) \times 10^{-13}\,(E/4\mathrm{TeV})^{-2.54\pm0.36}$ photons $\mathrm{cm}^{-2}\,\mathrm{s}^{-1}\,\mathrm{TeV}^{-1}$, in the energy range $1 \div 20$ TeV (see Fig. 1). The measured γ-ray flux is consistent with the Milagro results, but is $\sim 2 \div 3$ times larger than the flux derived by HESS at energies of a few TeV. Given the reduced significance of the excess at high energies, we are not able to constrain the shape of the spectrum above 10 TeV and to definitively rule out a possible high energy cutoff.

The continuity of the Milagro and ARGO-YBJ observations and the stable excess rate observed by ARGO-YBJ throughout 4 years of data collecting support the identification of MGRO J1908+06 as a stable extended source, likely the TeV nebula of PSR J1907+0602, with a flux at 1 TeV $\sim 67\,\%$ that of the Crab Nebula. Assuming a distance of 3.2 kpc, the integrated luminosity above 1 TeV is ~ 1.8 times that of the Crab Nebula, making MGRO J1908+06 one of the most luminous Galactic γ-ray sources at TeV energies [18].

2.5. MGRO J2031+41 and the Cygnus region

The Cygnus region contains a large column density of interstellar gas and is rich in potential CR acceleration sites as Wolf–Rayet stars, OB associations and supernova remnants. Several VHE γ-ray sources have been discovered within this region in the past decade, including two bright extended sources detected by the Milagro experiment.

The γ-ray source MGRO J2031+41, detected by Milagro at a median energy of ~ 20 TeV, is spatially consistent with the source TeV J2032+4130 discovered by the HEGRA collaboration and likely associated with the Fermi pulsar 1FGL J2032.2+4127. The extension measured by Milagro, $3.0° \pm 0.9°$, is much larger than that initially estimated by HEGRA (about 0.1°).

The bright unidentified source MGRO J2019+37 is the most significant source in the Milagro data set, apart from the Crab Nebula. This is an enigmatic source, due to its high flux not being confirmed by other VHE γ-ray detectors. Recently, a deep survey carried out by VERITAS with sensitivity of $\sim 1\,\%$ Crab units showed a complex emitting region with different faint sources inside the MGRO J2019+37 extension. The estimated flux is much weaker than that determined by Milagro.

The Cygnus region has been studied by ARGO-YBJ with data collected in a total effective observation time of 1182 days [19]. The results of the data analysis are shown in Figs. 2 and 3. A TeV emission from a position consistent with MGRO J2031+41/TeV J2032+4130 is found with a significance of 6.4 s.d. Assuming the background spectral index −2.8, the intrinsic extension is determined to be $\sigma_{\rm ext} = (0.2^{+0.4}_{-0.2})°$, consistent with the estimation by the MAGIC and HEGRA experiments, i.e., $(0.083 \pm 0.030)°$ and $(0.103 \pm 0.025)°$, respectively.

The differential flux is $\mathrm{d}N/\mathrm{d}E = (1.40 \pm 0.34) \times 10^{-11}\,(E/\mathrm{TeV})^{-2.83\pm0.37}$ $\mathrm{ph\,cm}^{-2}\,\mathrm{s}^{-1}\,\mathrm{TeV}^{-1}$ (Fig. 3), in the energy range $0.6 \div 7$ TeV. Assuming $\sigma_{\rm ext} = 0.1$, the integral flux is 31 % that of the Crab at energies above 1 TeV, which is higher than the flux of TeV J2032+4130 as determined by HEGRA (5 %) and

MAGIC (3 %). Again, this measurement is in fair agreement with the Milagro result.

The reason for the large discrepancy between the fluxes measured by Cherenkov telescopes and by EAS arrays (ARGO-YBJ and Milagro) is still unclear. Possible contributions from diffuse γ-ray emission, nearby sources, and systematic uncertainties are not enough to explain the discrepancy [19].

No evidence of a TeV emission above 3 s.d. is found at the location of MGRO J2019+37, and flux upper limits at 90 % c.l. are set. At energies above 5 TeV, the ARGO-YBJ exposure is still insufficient to reach a firm conclusion, while at lower energies the ARGO-YBJ upper limit is marginally consistent with the spectrum determined by Milagro. The observation by ARGO-YBJ is about five years later than that by Milagro. A flux variation over the whole extended region cannot be completely excluded. If the flux variation were dominated by a smaller region in the source area, the picture could be more reasonable. In such a scenario, however, identifying MGRO J2019+37 as a PWN could be a dilemma, because it otherwise should have a steady flux.

3. Cosmic Ray Physics

Several interesting results have been obtained by ARGO-YBJ in CR physics, as discussed in [3]. In the following sections, measurements of the anisotropy in the CR arrival direction distribution and of the light component (p + He) spectrum of CRs are described.

3.1. Large Scale CR Anisotropy

The observation of the CR large scale anisotropy by ARGO-YBJ is shown in Fig. 4 as a function of the primary energy up to about 25 TeV.

The so-called *'tail-in'* and *'loss-cone'* regions, correlated to an enhancement and a deficit of CRs, respectively, are clearly visible with statistical significance greater than 20 s.d. The tail-in broad structure appears to break up into smaller spots with increasing energy. In order to quantify the scale of the anisotropy we studied the 1-D R.A. projections integrating the sky maps inside a declination band given by the field of view of the detector. For this, we fitted the R.A. profiles with the first two harmonics. The resulting amplitude and phase of the first harmonic are plotted in Figs. 5 and 6, where they are compared to other measurements as a function of the energy. The ARGO-YBJ results are in agreement with those of other experiments, suggesting a decrease of the anisotropy first harmonic amplitude at energies above 10 TeV.

3.2. Medium Scale Anisotropy

Figure 7 shows the ARGO-YBJ sky map in equatorial coordinates containing about 2×10^{11} events reconstructed with a zenith angle $\leq 50°$.

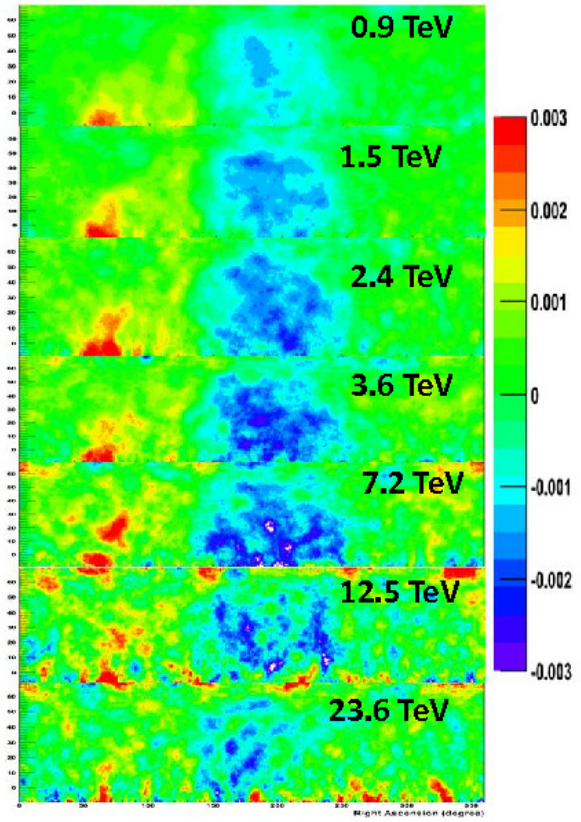

Figure 4. Large scale CR anisotropy observed by ARGO-YBJ as a function of the energy. The color scale gives the relative CR intensity.

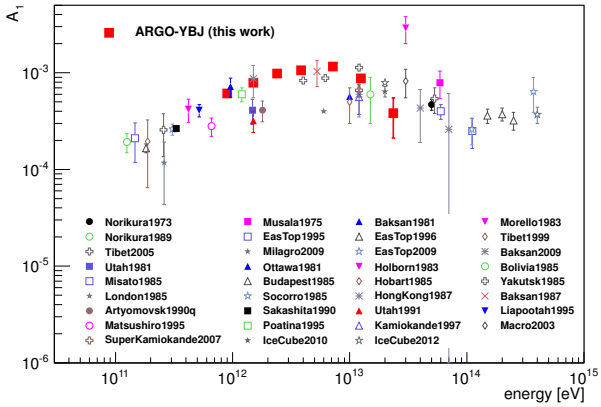

Figure 5. Amplitude of the first harmonic as a function of the energy, compared with other measurements.

The zenith cut selects the declination region $\delta \sim -20° \div 80°$. According to simulations, the median energy of the isotropic CR proton flux is $E_p^{50} \approx 1.8$ TeV (mode energy ≈ 0.7 TeV).

The most evident features are observed by ARGO-YBJ around the positions $\alpha \sim 120°$, $\delta \sim 40°$ and $\alpha \sim 60°$, $\delta \sim -5°$, positionally coincident with the excesses detected by Milagro [20]. These regions, named "1" and "2", are observed with a statistical significance of about 14 s.d. The deficit regions parallel to the ex-

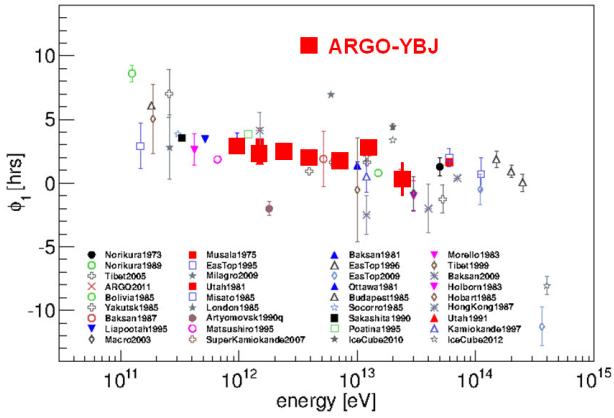

Figure 6. Phase of the first harmonic as a function of the energy, compared with other measurements.

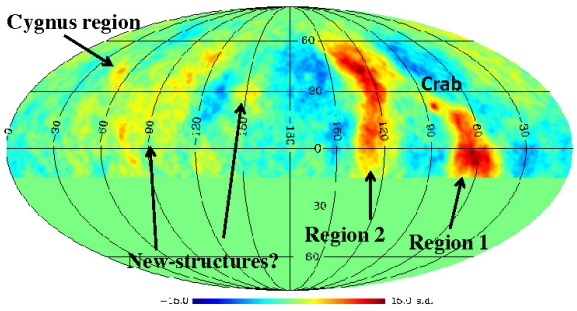

Figure 7. Medium scale CR anisotropy observed by ARGO-YBJ. The color scale gives the statistical significance of the observation in standard deviations.

cesses are due to a known effect of the analysis, which uses also the excess events to evaluate the background, overestimating this latter.

The left side of the sky map seems to be full of few-degree excesses not compatible with random fluctuations (the statistical significance is more than 6 s.d. post-trial). The observation of these structures is reported here for the first time and together with that of regions 1 and 2 it may open the way to an interesting study of the TeV CR sky.

To figure out the energy spectrum of the excesses, the data have been divided into five independent shower multiplicity sets. The number of events collected within each region is computed for the event map (Ev) as well as for the background map (Bg). The relative excess (Ev − Bg)/Bg is computed for each multiplicity interval.

The result is shown in Fig. 8. Region 1 seems to have a spectrum harder than isotropic CRs and a cutoff around 600 shower particles (proton median energy $E_{\rm p}^{50} = 8\,\mathrm{TeV}$). On the other hand, the excess hosted in region 2 is less intense and seems to have a spectrum more similar to that of isotropic CRs. We point out that, in order to filter the global anisotropy, we used a method similar to that used by Milagro and Icecube. Further studies using different approaches are under way.

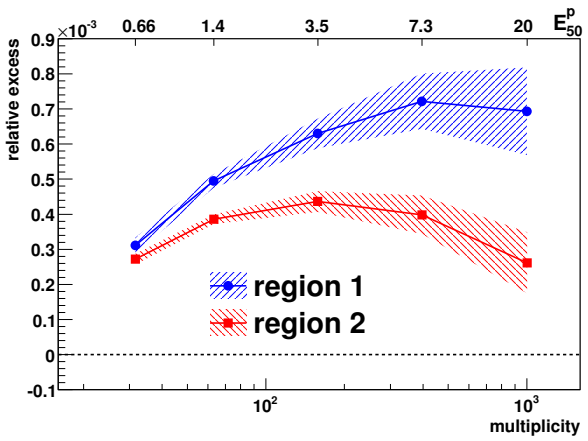

Figure 8. Size spectrum of regions 1 and 2. The vertical axis represents the relative excess (Ev − Bg)/Bg. The upper scale shows the corresponding proton median energy. The shadowed areas represent the 1σ error band.

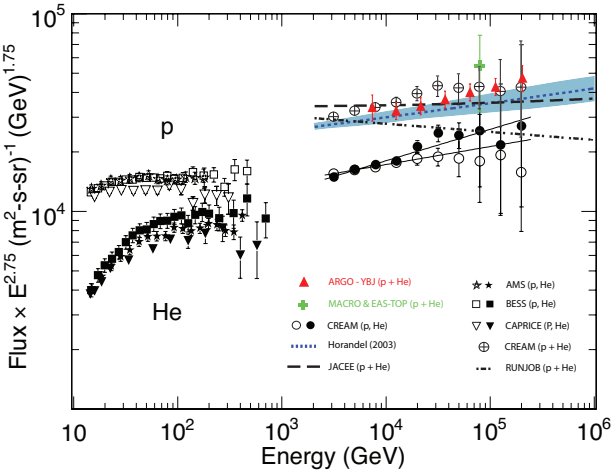

Figure 9. Light component (p + He) spectrum of primary CRs measured by ARGO-YBJ compared with other experimental results.

3.3. Light component (p + He) spectrum of CRs

Requiring quasi-vertical showers ($\theta < 30°$) and applying a selection criterion based on particle density, a sample of events mainly induced by protons and helium nuclei with the shower cores inside a fiducial area (with radius $\sim 28\,\mathrm{m}$) has been selected. The contamination by heavier nuclei is found to be negligible. An unfolding technique based on the Bayesian approach has been applied to the strip multiplicity distribution in order to obtain the differential energy spectrum of the light component (p + He nuclei) in the energy range $(5 \div 200)\,\mathrm{TeV}$ [23]. The spectrum measured by ARGO-YBJ is compared with other experimental results in Fig. 9. Systematic effects due to different hadronic models and due to the selection criteria do not exceed 10 %. The ARGO-YBJ data agree remarkably well with the values obtained by adding up the p and He fluxes measured by CREAM,

concerning both the total intensities and the spectral index [21]. The value of the spectral index of the power-law fit to the ARGO-YBJ data is -2.61 ± 0.04, which should be compared with $\gamma_p = -2.66 \pm 0.02$ and $\gamma_{He} = -2.58 \pm 0.02$ obtained by CREAM. The present analysis does not allow the determination of the individual p and He contribution to the measured flux, but the ARGO-YBJ data clearly exclude the RUNJOB results [22]. We emphasize that for the first time direct and ground-based measurements overlap for a wide energy range thus making it possible to cross-calibrate the different experimental techniques.

4. Conclusions

The ARGO-YBJ detector exploiting the full coverage approach and the high segmentation of the readout is imaging the front of atmospheric showers with unprecedented resolution and detail. The digital and analog readout will allow a deep study of the CR phenomenology in the wide TeV $\div$ PeV energy range. The results obtained in the low energy range (below 100 TeV) predict an excellent capability to address a wide range of important issues in Astroparticle Physics.

References

[1] Aielli, G. et al.: 2006, NIM A562, 92

[2] Bartoli, B. et al.: 2011a, Phys. Rev. D84, 022003

[3] D'Ettorre Piazzoli, B.: 2011, in *32nd ICRC Proc.*, Highlight talk

[4] Aielli, G. et al.: 2010a, ApJ 714, L208

[5] Bartoli, B. et al.: 2011b, ApJ 734, 110

[6] Tavani, M. et al.: 2011, Science 331, 736

[7] Abdo, A.A. et al. 2011, Science 331, 739

[8] Striani, E. et al.: 2011, arXiv:1105.5028

[9] Ojha R. et al.: 2012, Astron. Telegram 4239

[10] Balbo, M. et al.: 2011, A&A 527, L4

[11] Aielli, G. et al.: 2010b, Astron. Telegram 2921

[12] Mariotti, M. et al.: 2010, Astron. Telegram 2967

[13] Ong, R. et al.: 2010, Astron. Telegram 2968

[14] Buehler, R. et al.: 2011, Astron. Telegram 3276

[15] Bartoli, B. et al.: 2012a, Astron. Telegram 4258

[16] Bartoli, B. et al.: 2011c, ApJ, 734, 110

[17] Bartoli, B. et al.: 2012b, ApJ in press

[18] Bartoli, B. et al.: 2012c, ApJ in press, arXiv:1207.6280

[19] Bartoli, B. et al.: 2012d, ApJL 745, L22

[20] Abdo, A.A. et al.: 2008, Phys. Rev. Lett. 101, 221101

[21] Yoon, Y.S. et al.: 2011, ApJ 728, 122

[22] Derbina V.A. et al.: 2005, ApJL 628, L41

[23] Bartoli, B. et al.: 2012e, Phys. Rev. D 85, 092005